Rapid Communications

# Spin-orbit interaction and spin selectivity for tunneling electron transfer in DNA

Solmar Varela,[1,*] Iskra Zambrano,[2] Bertrand Berche,[3] Vladimiro Mujica,[4] and Ernesto Medina[2,5,†]

[1]*Yachay Tech University, School of Chemical Sciences & Engineering, 100119-Urcuquí, Ecuador*

[2]*Yachay Tech University, School of Physical Sciences & Nanotechnology, 100119-Urcuquí, Ecuador*

[3]*Laboratoire de Physique et Chimie Théoriques, UMR Université de Lorraine-CNRS 7019 54506 Vandœuvre les Nancy, France*

[4]*School of Molecular Sciences, Arizona State University, Tempe, Arizona 85287-1604, USA*

[5]*Simon A. Levin Mathematical, Computational and Modeling Sciences Center, Arizona State University, Tempe, Arizona 85287-1604, USA*

(Received 26 January 2020; revised manuscript received 27 April 2020; accepted 14 April 2020; published 11 June 2020)

Electron transfer (ET) in biological molecules, such as peptides and proteins, consists of electrons moving between well-defined localized states (donors to acceptors) through a tunneling process. Here, we present an analytical model for ET by tunneling in DNA in the presence of spin-orbit (SO) interaction to produce a strong spin asymmetry with the intrinsic atomic SO strength in the meV range. We obtain a Hamiltonian consistent with charge transport through $\pi$ orbitals on the DNA bases and derive the behavior of ET as a function of the injection state momentum, the spin-orbit coupling, and barrier length and strength. Both tunneling energies, deep below the barrier and close to the barrier height, are considered. A highly consistent scenario arises where two concomitant mechanisms for spin selection arises; spin interference and differential spin amplitude decay. High spin filtering can take place at the cost of reduced amplitude transmission assuming realistic values for the SO coupling. The spin filtering scenario is completed by addressing the spin-dependent torque under the barrier with a consistent conserved definition for the spin current.

DOI: 10.1103/PhysRevB.101.241410

Extensive studies show that electronic transfer in biological systems (for example, photosynthesis and respiration [1]) is fast and efficient, which can be explained by means of tunneling processes through organic molecules [1,2]. Hopfield [3], Beratan [4,5] were some of the first who developed a theory in terms of electron tunneling through a barrier to analyze the electronic transfer in biological systems. In addition, they showed that the dependence on distance in proteins is related to their structure and that tunneling is mediated by consecutive electronic interactions between connecting donors with acceptor sites. Electron transfer by pure quantum tunneling has been shown to occur over distances between 20 and 40 Å [6,7] in biological molecules, such as proteins and DNA or $\pi$-conjugated structures. Such processes are temperature insensitive indicating that they are not activated and are partially coherent [8].

Tunneling processes coupled to spin activity have been modeled previously when time-reversal symmetry is broken. Büttiker [9] proposed a model for a spin active barrier, that considers a magnetic field in the barrier region, to study the polarization of the transmitted waves and the characteristic dwell times for each spin component. Such an approach suggests a similar mechanism might be relevant for the spin-orbit (SO) coupled (time-reversal preserving) chiral-induced spin selectivity (CISS) effect [10–13]. Spin active tunneling in chiral molecules has not received deserved attention despite its relevance in molecular systems. Recently, Michaeli and Naaman [14] considered tunneling through the dipole potential produced by hydrogen bonding in a helical geometry. This model is akin to both DNA and oligopeptides with $\alpha$ helices, that are strong spin polarizers. Nevertheless, their model did not discuss the details of tunneling coupled to the SO interaction, each spin component propagating equally through the dipole barrier.

Here, we propose to extend the Büttiker model to the detailed spin-orbit Hamiltonian previously concocted for DNA [15]. The model assumes a small doping by either electrons or holes, through the surface-molecule contact, rendering the SO coupling linear in $k$. We find that the energy splitting associated with the spin-orbit term generates different decay rates for each spin species. The different rates produce an exponentially large polarization effect albeit that the coupling is in the meV range [16]. This large effect frees the theory from the need of unphysically large SO coupling to yield the experimentally observed polarization results while making additional predictions on polarization rates. An estimate of the torque dipoles in the molecule due to the SO coupling is consistent with the previous picture.

The full model Hamiltonian for B-DNA in a repeated sequence incorporating the Stark effect for the electric fields connecting the bases of the molecule and atomic spin-orbit coupling has been derived recently by Varela *et al.* [15] and Varela *et al.* [16]. The model involves the orbital basis $\{p_x, p_y, p_z, s\}$ on each base, on a double stranded helix, assuming weak coupling to the partner strand. Figure 1 shows the $\pi$-stacking model [17], showing only a single $p_z$ orbital standing from each base. The wave function overlaps, and SO couplings are derived from a tight-binding

*svarela@yachaytech.edu.ec

†emedina@yachaytech.edu.ec

 

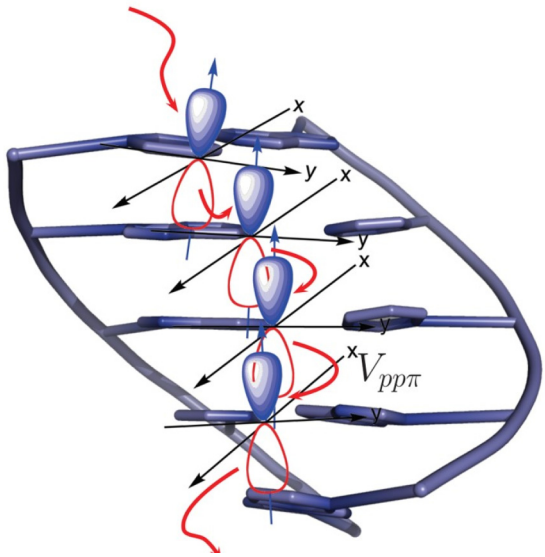


FIG. 1. Orbital model for transport in DNA. The figure depicts the electron carrying orbitals ($p_z$ orbital perpendicular to the base planes) coupled by $V_{pp\pi}$ Slater-Koster matrix elements.

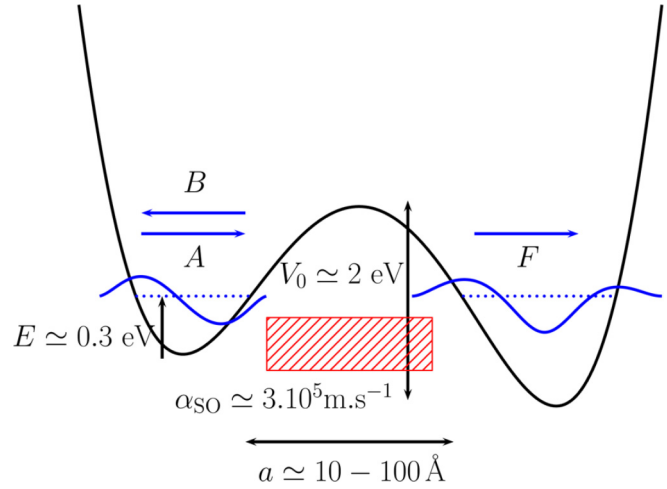


FIG. 2. Scattering potential barrier model with SO interaction (red hatch). The label for the incident ($A$) and scattered ($B$ and $F$) wave-function amplitudes are indicated. The well parameters are estimated in the text on the basis of polaron transport.

Slater-Koster analytical approach with lowest-order perturbation theory [15].

The Fermi level for one orbital assumes half-filling, whereas light doping of the molecule by electrons or holes, e.g., from contact with a substrate, determines the dispersion relation around the Fermi energy. On the molecule, the mobile electrons in the bases, thus, come from $\pi$ orbitals [18]. Although these orbitals may be thought of as fully filled, interactions with neighboring bases and a surrounding environment will transfer electrons, a process that we model as a change in the filling of these orbitals.

The largest contributions to the Hamiltonian, considering only the intrinsic spin-orbit coupling of atoms involved in $\pi$ orbitals ($N$, $C$, and $O$), comprises two terms,

$$H = [\varepsilon_{2p}^{\pi} + 2t f(k)]\mathbf{1}_s - 2g(k)\lambda_{SO}\boldsymbol{s}_y, \tag{1}$$

where $\mathbf{1}_s$ represents the unit matrix in spin space and $\boldsymbol{s}_y$ is the spin degree of freedom in the local coordinate system of the molecule. The first term in the Hamiltonian (1), involves the base $2p-\pi$ orbital energy ($\varepsilon_{2p}^{\pi}$). The kinetic-energy $t(r,b)$ depends explicitly on the structural parameters of the molecule [15], where $r$ and $b$ are the radius and pitch of the helix. The second term in (1), contains the spin active term $\lambda_{SO}(r,b,\xi_p)$, depending also on the helix orbital overlaps and local energies, where $\xi_p$ is the atomic SO coupling of double bonded atoms in the bases ($C$, $O$, or $N$). The $\lambda_{SO}$ parameter also includes all geometrical overlaps characteristic of the helix. Finally, $f(k) = \cos(\boldsymbol{k}\cdot\boldsymbol{R})$ and $g(k) = \sin(\boldsymbol{k}\cdot\boldsymbol{R})$ are the functions of reciprocal space with $R$ as the lattice parameter and $k$ as the wave vector in the local system of the helix. This Hamiltonian only includes the dominant spin active terms derived from the geometry-dependent spin-orbit coupling.

Charge transfer/doping by the environment of the molecule or by the substrate on which the molecule is attached, can add or subtract charge shifting the dispersion from the inflection point $K_\mu$ for the purely kinetic Hamiltonian. Thus, the Fermi energy corresponds to $K_\mu = 0$ so that $k = K_\mu + q$ describes a perturbative doping in the vicinity of the Fermi level. Expanding to lowest order in $q$ and assuming that $\boldsymbol{k}\cdot\boldsymbol{R} \ll 1$, we have

$$\begin{aligned} f(k) &= 1 - \frac{q^2R^2}{2} + O(q^4)\ldots, \\ g(k) &= qR + O(q^3)\ldots, \end{aligned} \tag{2}$$

and the resulting Hamiltonian is as follows:

$$H = \left[\varepsilon_{2p}^{\pi} + 2t\left(1 - \frac{q^2R^2}{2}\right)\right]\mathbf{1}_s - 2qR\lambda_{SO}\boldsymbol{s}_y. \tag{3}$$

In the sense of $kp$ theory [19], we can requantize this Hamiltonian to treat the tunneling problem in the vicinity of the Fermi level: $q \longrightarrow -i\partial_x$ and $\hbar^2/2R^2|t| \longrightarrow m$. Eliminating constant energy terms (uniform sequence assumption), we arrive at

$$H = \frac{1}{2m}(-i\hbar\partial_x)^2\mathbf{1} + \alpha\sigma_y(-i\hbar\partial_x), \tag{4}$$

where $\alpha = -R\lambda_{SO}$ and $\sigma_y$ is the Pauli matrix. This derivation results in the same Hamiltonian surmised in Ref. [20] and leads to the detailed physics of the CISS effect in the absence of tunneling. The Hamiltonian in Refs. [15,21] can then be considered as a microscopic derivation of the continuum description.

We now introduce the previous model under a potential barrier assuming as shown in Fig. 2 that electrons are injected from (and partially reflected back to) a donor localized state and received at an acceptor site. One might also consider dipole barriers as expected from the hydrogen bond generated potential identified in Ref. [14]. We consider an incident state of momentum $p_x$, where $x$ is along the helix tangent. Electrons interact with a potential barrier of height $V_0$ and width $a$. In the barrier region, the SO interaction is active (see Fig. 2 and

Ref. [22]). The scattering problem is then defined by

$$H = \begin{cases} \left(\frac{p_x^2}{2m} + V_o\right)\mathbf{1} + \alpha\sigma_y p_x, & 0 \leqslant x \leqslant a, \\ \text{donor/acceptor states}, & \text{outside}. \end{cases} \quad (5)$$

The parameters used for the injected momentum, barrier height, and the range of spin-orbit values are selected as follows: electron transfer from experimental techniques based on coupling artificial donor and acceptor sites has been tested using a series of well-conjugated molecules including metallointercalators, organic intercalators, and organic end cappers [23]. Measurements, using DNA as a bridge, report tunneling between 10 and 40 Å [6,7,24,25]. On the other hand, the barrier heights reported are in the range of 0.5–2.5 eV [26,27], either by the potential difference between the metal intercalators as donors/acceptors or the substrate in a scanning tunneling microscope (STM) setup and the highest occupied molecular orbital state of guanine [28].

The donor confinement potential can give an idea of the approximate $k$-vector values being injected into the barrier, assuming carriers are in the ground state. Intercalators, such as those in Ref. [25] or STM setups [8] report confinement over one or two base pairs. We can estimate in the range of $k = 0.4\ \text{nm}^{-1}$, corresponding to the incident energy of $E = 0.24$ and $V_0 = 2$ eV. With these experimentally derived parameters, we can see the consequences of differential spin tunneling with the derived Hamiltonian.

Using the estimated barrier parameters and the polaron well parameters, we can fully solve the one-dimensional scattering problem by assuming an initial pure spin state. To determine the scattering properties, we can solve the problem with simple plane-wave injection conditions. The Hamiltonian $H$ acts on spinors $\psi$ with the form $\psi(x) = [\psi_\uparrow(x), \psi_\downarrow(x)]$ where the arrows indicate the spin components. If the incident beam is given by $\psi_{in}(x) = (A_\uparrow, A_\downarrow)e^{ikx}$ and the spinor for the scattered beam is $\psi_{in}(x) = (F_\uparrow, F_\downarrow)e^{ikx}$ then, the spin asymmetry of the scattered beam cam be written in the form $P_z = (|F_\uparrow|^2 - |F_\downarrow|^2)/(|F_\uparrow|^2 + |F_\downarrow|^2)$.

Considering an incident electron with energy $E$ and wave-vector $k$, the general solutions are $\psi_1 = (A_\uparrow, A_\downarrow)e^{ik_1 x} + (B_\uparrow, B_\downarrow)e^{-ik_1 x}$ for $x \leqslant 0$ and $\psi_3 = (F_\uparrow, F_\downarrow)e^{ik_3 x}$ for $x \geqslant a$ and in the region of the barrier, the general solution is

$$\psi_2 = \begin{pmatrix} C_\uparrow e^{iq_\uparrow x} \\ C_\downarrow e^{iq_\downarrow x} \end{pmatrix} + \begin{pmatrix} D_\uparrow e^{-iq_\uparrow x} \\ D_\downarrow e^{-iq_\downarrow x} \end{pmatrix}, \quad 0 \leqslant x \leqslant a \ , \quad (6)$$

where $C$ and $D$ are the corresponding amplitudes.

Solving the eigenvalue problem $H\psi = E\psi$ for each of the regions, we have that wave vectors for the electron in 1 and 3 are $k_1 = k_3 = \sqrt{2mE}/\hbar$ and for region 2, the wave-vector $q$ depends on the spin orientation and is given by

$$q_s = \sqrt{k^2 - q_0^2 + \left(\frac{m\alpha}{\hbar}\right)^2} + s\left(\frac{m\alpha}{\hbar}\right), \quad (7)$$

where $q_0^2 = 2mV_0/\hbar^2$, $k^2 = 2mE/\hbar^2$. $s$ is the label associated with the spin up(down) such that $s = +(-)$. One can see the explicit dependence of $q$ with the spin $s$, $V_0$ and with the SO magnitude $\alpha$. Note that, if $E > V_0$, then wave-vector $q_s$ in the barrier region is real and the amplitudes will oscillate due to standing-wave patterns between the edges of the barrier and the spin precession (relative changes in the spinor amplitudes) due to the SO coupling. On the other hand, if $E < V_0$, then $q$ is, in general, a complex quantity, and the behavior of the general solution given by Eq. (6) will depend of the relation of $\alpha$, $k$, and $V_0$ values.

The coefficients are determined by the requirement of the continuity of the wave function at $x = 0$ and $x = a$ following Ref. [29]: $\psi_{1,s}(0) = \psi_{2,s}(0)$, $\psi_{2,s}(a) = \psi_{3,s}(a)$ and $\hat{v}_{x,1}\psi_1(0) = \hat{v}_{x,2}\psi_2(0)$, $\hat{v}_{x,2}\psi_2(a) = \hat{v}_{x,3}\psi_3(a)$ where the velocity in the corresponding regions is derived from $\hat{v}_x = \partial H/\partial p_x$.

Below the barrier transmission, will be the most common physical scenario where we have an interplay among three energies: (i) the incoming energy of the electron estimated by the quantum well that precedes the barrier, (ii) the barrier height $V_0$, and (iii) the SO energy that has been estimated to be in the meV range [16]. It is useful to consider some possible values of the wave vector inside barrier $q_s$ [Eq. (7) with $k < q_0$]:

(1) $\alpha = 0$, $q_s = \sqrt{|q_0^2 - k^2|}$, and no spin activity is expected. Simple wave-function decay is expected.

(2) $|q_0^2 - k^2| > (m\alpha/\hbar)^2$, then $q_s$ will be a complex number ($\alpha \neq 0$). Then, we have an underdamped decay of the barrier wave function.

(3) If $|q_0^2 - k^2| < (m\alpha/\hbar)^2$, then $q_s$ is a purely imaginary number, and the wave function is a plane wave.

When the spin-orbit energy $E_{SO}$ approaches $|\hbar^2 k^2/2m - V_0|$, a transition is expected between the latter two regimes.

All previous regimes are depicted in Fig. 3 for the polarization as a function of the barrier length and the SO parameter $m\alpha^2/2$. The range chosen for the SO energy is in agreement with the values computed in Ref. [16]. Figure 3(a) shows the situation deep below the barrier where the wave function oscillates and decays. At finite $\alpha$, there is an exponential growth of the polarization compounded by interference effects due to different oscillation frequencies of the $|\uparrow, \downarrow\rangle$ spin components. This gives a reentrant effect where polarization can increase and then decrease as a function of the barrier width. Note the polarization can increase a factor of 3 for a change in between 0.1 and 1 nm in barrier length. At 1-nm barrier length and 40-meV Rashba coupling [30], we find a polarization of 30%.

Spin filtering by tunneling in spin active media generates a high polarization with the expected molecular SO coupling, but the amplitude is also exponentially small. Experimental accounts for the polarization rates [31] should be able to check for this feature in time-resolved experiments or essays that can change the tunneling length by, e.g., mechanical stretching [16,32]. Figure 3(b) depicts a different regime where one has an input energy close to the barrier height. There we see a stronger reentrant effect that extends for even lower values of the SO energy while increasing the needed barrier lengths for the same polarization enhancement as in Fig. 3(a). Finally, Fig. 3(c) shows the sensitivity of the barrier-polarizing strength as a function of the input momentum. The figure also shows the possibility of tuning the well-associated momentum and the barrier length to achieve large filtering efficiencies.

It has been shown that, in the presence of SO coupling, the conventional definition of spin current as a matrix element of

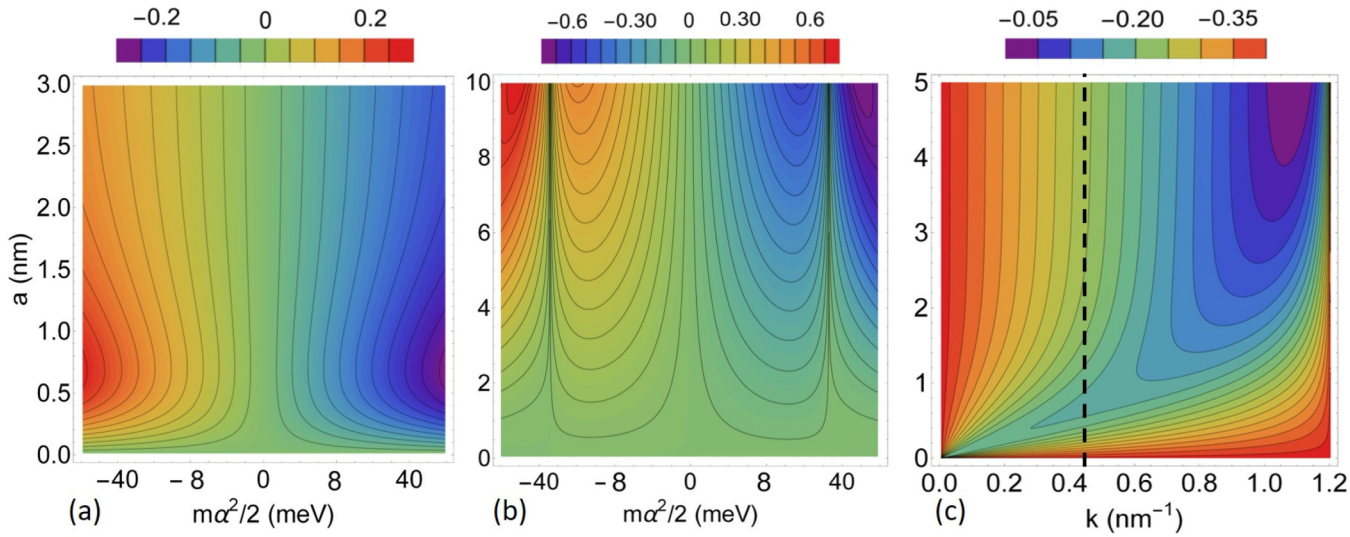


FIG. 3. Spin asymmetry $P_z$ as a function of barrier length $a$ in nanometers and the energy of the SO interaction with fixed values for the incident wave function of electron and the barrier height: (a) $k = 0.44\ \text{nm}^{-1}$, $q_0 = 1.2\ \text{nm}^{-1}$ deep under the barrier; (b) $k = 0.44\ \text{nm}^{-1}$, $q_0 = 0.46\ \text{nm}^{-1}$ close to the top of the barrier. Panel (c) shows the spin asymmetry $P_z$ versus $a$, and the input momentum $k$ with $q_0 = 1.2\ \text{nm}^{-1}$ and $m\alpha^2/2 = 30$ meV are fixed. The dotted line represents a reasonable value for $k$ argued in the text.

$\hat{\mathbf{J}}_\mathbf{s} = (1/i\hbar)\{\mathbf{v}, s_z\}$ is incomplete and unphysical [33,34]. The consistent spin current density should be written in the form [33]

$$\mathfrak{I}_s = \text{Re}\,\Psi^\dagger(\vec{r})\hat{\mathfrak{I}}_s\Psi(\vec{r}), \tag{8}$$

where $\hat{\mathfrak{I}}_s = d(\hat{r}\hat{s}_z)/dt$ is the effective spin current operator and $\Psi(\vec{r})$ is the spatially dependent wave function. The previous operator can be easily shown to be $\hat{\mathfrak{I}}_s = \hat{\mathbf{J}}_\mathbf{s} + \hat{\mathbf{P}}_\tau$ where $\hat{\mathbf{J}}_\mathbf{s}$ is the conventional spin current operator, and the extra term $\hat{\mathbf{P}}_\tau$ is the torque dipole density from the corresponding torque density $\tau$ due to the presence of the SO coupling. Considering our Hamiltonian (5), $\hat{\mathbf{J}}_\mathbf{s}$ and $\hat{\mathbf{P}}_\tau$ are readily accessible. The torque density can be then computed by the relation,

$$\mathcal{T}_\mathbf{s} = \text{Re}\left\{\Psi^\dagger \frac{1}{i\hbar}[\hat{s}_z, \hat{H}]\Psi\right\} = \nabla\cdot\mathbf{P}_s. \tag{9}$$

Figure 4 shows the torque density integrated over the barrier length as a function of physical values for the SO energy. The figure shows the range where there is a torque differential between spin species producing the net spin polarization seen previously. The sharp dip indicates the SO coupling that produces pure wave behavior under the barrier [see Eq. (7)]. It is notable (see the inset), there is no linear regime for small $\alpha$ that shows spin polarization. One can think of torques taking away angular momentum, depending on the spin species, as the mechanism for generating spin polarization under the barrier. This is a clear insight derived from the consistent formulation of the conserved spin current definition [33,34].

As a concrete estimate of the change in angular momentum produced by the torque density: Using the input $k$-vector range in Fig. 3(c), we can estimate the barrier dwell time [9] for $k = 0.44\ \text{nm}^{-1}$ is $10^{-14}$ (see Ref. [35]). From this estimate, we can compute, from Fig. 4, that the total change in angular momentum is $\Delta L \sim 0.1\hbar/2$. This is a polarization that is comparable to that reported in Fig. 3(c).

We have derived a Hamiltonian for a model of doped DNA including the SO coupling term that depends linearly on crystal momentum. We assume that electrons tunnel under a barrier of length $a$ between confined electron-phonon/polaron states. The SO couples differently to each component of the spinor yielding a net spin-polarized output. The output polarization can be very large, e.g., 60% for realistic values of the SO coupling [16], depending on the relation between the barrier length and the input $k$ vector of the electron. This is at the cost of a small spin current amplitude. We have also discussed the source of spin polarization as due to the existence of a torque density that differentiates between up and down spins using a consistent formulation of the spin current [33]. This mechanism is checked with an estimate of the change in angular momentum of the electron this torque density produces. Thus, there is no need to invoke

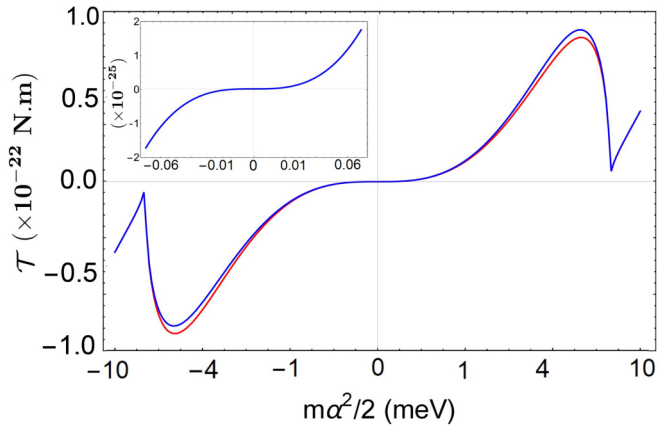


FIG. 4. Torque density $\tau_2$ in region 2 for the two spin components as a function of the SO coupling energy with $k = 0.440\ \text{nm}^{-1}$, $q_0 = 0.446\ \text{nm}^{-1}$, and $a = 5$ nm. Note there is no linear regime (see the inset) for spin filtering.

large unphysical SO strengths to achieve large experimental polarization values. Our results seem to offer an alternative interpretation to models that require time-reversal symmetry breaking, e.g., wave-function leakage to explain spin polarization in the context of the CISS effect [36,37]. We believe the model addressed here is valid for general sequences of DNA and oligopeptides as long as transport the mechanism involves short-range tunneling [8,38,39]. Nevertheless, nonuniform sequences would also introduce structure under the barrier, and thermal hopping and variable range hopping mechanism take over transport [40]. It is an interesting prospect to analyze spin filtering in this regime.

This work was supported by CEPRA VIII Grant No. XII-2108-06, *Mechanical Spectroscopy* funded by CEDIA, Ecuador. V.M. acknowledges a Fellowship from Ikerbasque, the Basque Foundation for Science. We acknowledge useful discussions with J. Svozilík.

[1] J. Winkler, A. Di Biblio, N. Farrow, J. Richards, and H. Gray, P. Appl. Chem. **71**, 1753 (1999).
[2] J. Blumberger, Chem. Rev. **115**, 11191 (2015).
[3] J. J. Hopfield, Proc. Nat. Acad. Sci. USA **71**, 3640 (1974).
[4] D. Beratan, J. N. Onuchic, and J. Hopfield, J. Chem. Phys. **86**, 4488 (1987).
[5] D. Beratan, J. N. Betts, and J. N. Onuchic, Science **252**, 1285 (1991).
[6] J. R. Winkler, A. R. Dunn, C. R. Hess, and H. B. Gray, *Electron Tunneling through Iron and Copper Proteins*, Bioinorganic Electrochemistry (Springer, The Netherlands, 2008).
[7] C. J. Murphy, M. R. Arkin, Y. Jenkins, N. D. Ghatlia, S. H. Bossmann, N. J. Turro, and J. K. Barton, Science **262**, 1025 (1993).
[8] L. Xiang, J. L. Palma, C. Bruot, V. Mujica, M. Ratner, and N. Tao, Nat. Chem. **7**, 221 (2015).
[9] M. Büttiker, Phys. Rev. B **27**, 6178 (1983).
[10] I. Carmeli, V. Skakalova, R. Naaman, and Z. Vager, Angew. Chem. Int. Edition **41**, 761 (2002).
[11] D. Mishra, T. Z. Markus, R. Naaman, M. Kettner, and B. Gohler, Proc. Natl. Acad. Sci. USA **110**, 14872 (2013).
[12] I. Carmeli, K. S. Kumar, O. Heifler, C. Carmeli, and R. Naaman, Angew. Chem., Int. Ed. **53**, 8953 (2014).
[13] Z. Xie, T. Z. Markus, S. Cohen, Z. Vager, R. Gutierrez, and R. Naaman, Nano Lett. **11**, 4652 (2011).
[14] K. Michaeli and R. Naaman, J. Phys. Chem. C **123**, 17043 (2019).
[15] S. Varela, V. Mujica, and E. Medina, Phys. Rev. B **93**, 155436 (2016).
[16] S. Varela, B. Montañes, F. Lopez, B. Berche, B. Guillot, V. Mujica, and E. Medina, J. Chem. Phys. **151**, 125102 (2019).
[17] J. C. Genereux and J. K. Barton, Chem. Rev. **110**, 1642 (2010).
[18] L. G. D. Hawke, G. Kalosakas, and C. Simserides, Mol. Phys. **107**, 1755 (2009); Eur. Phys. J. E **32**, 291 (2010).
[19] R. Winkler, *Spin-Orbit Coupling Effect in Two-Dimensional Electron and Hole Systems* (Springer-Verlag, Berlin/Heidelberg, 2003).
[20] E. Medina, L. A. Gonzalez-Arraga, D. Finkelstein-Shapiro, B. Berche, and V. Mujica, J. Chem. Phys. **142**, 194308 (2015).
[21] M. Geyer, R. Gutierrez, V. Mujica, and G. Cuniberti, J. Phys. Chem. C **123**, 27230 (2019).
[22] P. H. Cribb, S. Nordholm, and N. S. Hush, Chem. Phys. **44**, 315 (1979).
[23] G. B. Schuster, *Long-Range Charge Transfer in DNA II*, Topics in Current Chemistry Series Vol. 237 (Springer, New York, 2004), p. 73
[24] S. Risser, D. Beratan, and T. Meade, J. Am. Chem. Soc. **115**, 2508 (1993).
[25] A. R. Arnold, M. A. Grodick, and J. K. Barton, Cell Chem. Biol. **23**, 183 (2016).
[26] E. Wierzbinski, R. Venkatramani, K. L. Davis, S. Bezer, J. Kong, Y. Xing, E. Borguet, C. Achim, D. N. Beratan, and D. H. Waldeck, ACS Nano **7**, 5391 (2013).
[27] N. V. Grib, D. A. Ryndyk, R. Gutierrez, and G. Cuniberti, J. Biophys. Chem. **1**, 77 (2010).
[28] E. Macia, F. Triozon, and S. Roche, Phys. Rev. B. **71**, 113106 (2005).
[29] L. W. Molenkamp, G. Schmidt, and G. E. W. Bauer, Phys. Rev. B **64**, 121202(R) (2001).
[30] The SO coupling is not capped by the atomic SO coupling because it is a combination of SO and Stark interactions [16] for DNA and oligopeptides).
[31] R. Naaman and D. Waldeck, Annu. Rev. Phys. Chem. **66**, 263 (2015).
[32] S. Varela, V. Mujica, and E. Medina, Chimia **72**, 411 (2018).
[33] J. Shi, P. Zhang, D. Xiao, and Q. Niu, Phys. Rev. Lett. **96**, 076604 (2006).
[34] N. Sasao, H. Okada, Y. Utsumi, O. Entin-Wohlman, and A. Aharony, J. Phys. Soc. Jpn. **88**, 064702 (2019).
[35] R. J. Behm, N. Garcia, and H. Rohrer, *Scanning Tunneling Microscopy and Related Methods*, NATO ASI Series E, Applied Science Vol. 184 (NATO, Brussels, Belgium, 1990).
[36] S. Matityahu, Y. Utsumi, A. Aharony, O. Entin-Wohlman, and C. A. Balseiro, Phys. Rev. B **93**, 075407 (2016).
[37] S. Matityahu, A. Aharony, O. Entin-Wohlman, and S. Katsumoto, Phys. Rev. B **87**, 205438 (2013).
[38] B. Giese, J. Amaudrut, A.-K. Kohler, M. Spormann, and S. Wessely, Nature (London) **412**, 318 (2001); A. Shah, B. Adhikari, S. Martic, A. Munir, S. Shahzad, K. Ahmad, and H.-B. Kraatz, Chem. Soc. Rev. **44**, 1015 (2015).
[39] T. Aqua, R. Naaman, and S. S. Daube, Langmuir **19**, 10573 (2003); M. J. Bröcker, J. M. L. Ho, G. M. Church, D. Söll, and P. O'Donoghue, Angew. Chem., Int. Ed. **53**, 1 (2014).
[40] V. L. Nguyen, B. Z. Spivak, and B. I. Shklovskii, JETP Lett. **41**, 42 (1986); E. Medina and M. Kardar, Phys. Rev. B **46**, 9984 (1992).